Effects of O_2 Concentration on the Rate and Selectivity in Oxidative Dehydrogenation of Ethane Catalyzed by Vanadium Oxide: Implications for O_2 Staging and Membrane Reactors

Toshio Waku,[†] Morris D. Argyle, Alexis T. Bell,* and Enrique Iglesia*

Chemical Sciences Division, E. O. Lawrence Berkeley National Laboratory, and Department of Chemical Engineering, University of California at Berkeley, Berkeley, California 94720

Staged-O_2 introduction and the effects of O_2 concentration on primary and secondary reactions were examined during oxidative dehydrogenation on V_2O_5/γ-Al_2O_3 containing predominately isolated monovanadates. Cofeed and staged-O_2 introduction modes led to similar ethane dehydrogenation and combustion rates, despite significant differences in the average O_2 concentrations, as expected from their zero-order O_2 dependences. The rate of ethene conversion to CO_x, however, was lower when O_2 coreactants were introduced gradually as ethane conversion increased. These effects reflect inhibition of homogeneous ethene combustion pathways, which in contrast with their heterogeneous counterparts show a positive dependence in O_2. Axial O_2 distribution using multiple injectors or membranes will therefore influence alkene yields only by decreasing homogeneous alkene oxidation rates. Homogeneous contributions are much smaller in large reactors, because catalyst-to-volume ratios are greater than those in laboratory reactors. Other oxidation reactions occurring via redox cycles with lattice oxygens as the most abundant intermediates are expected to exhibit a response similar to that of O_2 staging.

Introduction

Many oxidation reactions on oxides occur via catalytic sequences requiring lattice oxygen atoms, as suggested first by Mars and van Krevelen for partial oxidation of aromatics on V_2O_5[1] and later confirmed for many oxidation reactions.[2−10] As a result, oxides can catalyze oxidation reactions even without gas-phase O_2, as long as lattice O atoms are available as stoichiometric coreactants.[1,5] Oxidative dehydrogenation (ODH) of alkanes involves such redox cycles and proceeds via the parallel and sequential pathways shown (Scheme 1).[2,9,10] Dehydrogenation (reaction 1) occurs in parallel with alkane conversion to CO and CO_2 (reaction 2), which also form in secondary alkene reactions (reaction 3). Rate constants for alkene combustion (k_3) are typically much larger than those for dehydrogenation (k_1), and maximum alkene yields are consequently low.[2,3,9,10]

These kinetic constraints and the need for alkene yield improvements have led to an extensive search for improved catalysts and for operating strategies that influence the relative rates of dehydrogenation and combustion. These steps appear to require similar types of sites, and their relative rates predominately depend on the relative C−H bond energies of alkanes and alkenes. Therefore, several studies have explored alternate approaches that minimize O_2 concentrations by separating the hydrocarbon and O_2 coreactants temporally or spatially, using cyclic and membrane reactors, respectively.

Vrieland and Murchison reported high C_4H_8 selectivity (~80%) at relatively high n-C_4H_{10} conversions (~50%) by alternate introduction of O_2/He and C_4H_{10}/He mixtures on MoO_3/MgO at 783 K.[5] Similar cyclic operation

Scheme 1. Primary and Secondary Reaction Pathways in ODH of Ethane
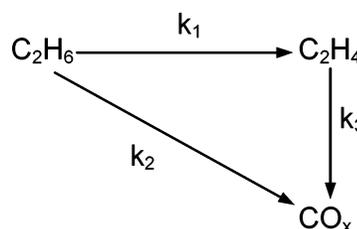
for C_3H_8 reactions led to high C_3H_6 selectivity (~80%) at low conversions (~5%) on V−Mg−O at 783−823 K[6,7] and to high C_3H_6 selectivity (~70%) at moderate conversions (<50%) on V−Si−O at 823 K.[8] In all three cases, it was suggested that the coexistence of hydrocarbons and O_2 led to undesired combustion reactions, even though lattice oxygens are involved in both selective and unselective pathways.

Lower O_2 concentrations can be maintained during steady-state ODH reactions in tubular reactors by staging the introduction of the required O_2 coreactant along the reactor. In this manner, the stoichiometric coreactant is supplied, but O_2 concentrations throughout the reactor length remain much lower than those in cofeed mode. In some cases, staging also allows the introduction of O_2 reactant requirements that would lead to explosive mixtures in cofeed mode. Oxygen transport membranes or multiple injection points can be used to implement these methods.[11−15] Membranes provide the additional advantage of separating O_2 from air, thus decreasing compression or reactor volume requirements. Tonkovich et al. reported 53% C_2H_4 selectivity at 95% C_2H_6 conversion using porous α-alumina membranes and $MgO/LiO/Sm_2O_3$ at 873 K; C_2H_4 selectivities were only 8% at similar conversion and temperature in a cofeed tubular reactor.[11] Wang et al. reported much higher C_2H_4 selectivity (80%) at 84%

C_2H_6 conversion at 1073 K using a mixed oxide ion conductor ($Ba_{0.5}Sr_{0.5}Co_{0.8}Fe_{0.2}O_{3-\delta}$) as the catalyst and membrane material than when the same catalyst was used in a cofeed reactor (54% selectivity).[12] Coronas et al. reported less marked improvements than Wang et al. for C_2H_6 ODH at 863−1013 K on Li/MgO using an inert membrane; they concluded that the minor effects observed reflected merely a more uniform axial temperature profile.[14]

Here, we explore the effects of O_2 staging during C_2H_6 ODH on VO_x/Al_2O_3 by exploiting the mathematical analogy between staged tubular reactors and semibatch recirculating reactors; these reactors allow significant procedural flexibility without the mechanical complexity of multiple injector or membrane reactors. In this manner, we aim to establish the feasibility of O_2 staging and of cyclic redox operating strategies in controlling desired and undesired pathways during alkane ODH reactions.

Experimental Methods

V_2O_5/γ-Al_2O_3 (2 wt % V_2O_5) was prepared by incipient-wetness impregnation of γ-Al_2O_3 (Degussa, AG, 100 m² g⁻¹) with a solution of ammonium metavanadate (99%, Aldrich, Inc.) and oxalic acid (Mallinckrodt A.G.).[10] The sample was dried in ambient air at 398 K for 16 h, crushed, treated in 1.67 cm³ s⁻¹(STP) dry air (Airgas zero grade) at 773 K for 3 h, and then sieved to retain 180−355 μm particles.[10]

O_2 cofeed and staging protocols were implemented for C_2H_6 ODH using a gradientless recirculating batch reactor.[16] V_2O_5/Al_2O_3 samples (0.10 g) were treated at 773 K in flowing 5% O_2/95% He (Praxair, C.P. >99.99%; 100 cm³ s⁻¹) for 1 h before catalytic experiments. C_2H_6 ODH rates and selectivities were measured at 743 K using ethane (16.0 kPa, Scott Specialty Gases, 99.999%) and two O_2 introduction protocols:

1. *Cofeed mode*: O_2 (12.0 kPa, Praxair, 99.999%) was added at the start of the experiment together with the C_2H_6 coreactant.

2. *Staged-feed mode*: O_2 (Praxair, 99.999%) was initially added at 1.0 kPa and introduced continuously [4.5 mmol (g-atom of V)⁻¹ s⁻¹] to maintain nearly constant O_2 concentrations as reaction occurred.

Reactants were introduced into the glass recirculating volume (520 cm³) after evacuation to <0.1 Pa. A graphite gear pump was used to circulate the reactor contents at >2 cm³ s⁻¹ to ensure gradientless operation and low conversion per pass (<1%).[17] Staged-O_2 experiments involved the continuous addition of O_2 during reaction using a glass capillary (60 m length, 250 μm diameter) at a flow rate controlled by the pressure at the capillary inlet. Homogeneous ethene combustion pathways were examined at 743 K in an empty reactor (2.0 cm³). Reactant mixtures consisted of C_2H_4 (16.0 kPa, Airgas Specialty Gases, Inc., 99.9%), and O_2 was introduced at 0.13 μmol s⁻¹ during homogeneous reactions.

Reactants and products were analyzed using gas chromatography (Hewlett-Packard, model 5890) with capillary (HP-1 methyl silicone column, 50 m, 320 μm) and packed (Supelco, 1000 Carboxen) columns and flame ionization and thermal conductivity detection. The amounts of products formed are reported as site yields [(moles of reactant converted to a given product)⁻¹ (g-atom of V)⁻¹]. Selectivities are given on a carbon basis based on the amount of ethane converted. Rate con-
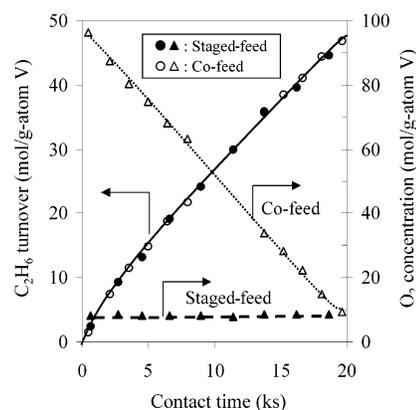
Figure 1. C_2H_6 turnovers (circles) during C_2H_6 ODH on 2 wt % V_2O_5/Al_2O_3 and O_2 concentration (triangles) in a gradientless batch reactor (743 K, 16.0 kPa C_2H_6, 12.0 kPa O_2 at cofeed mode; 1.0 kPa and 4.5 mmol of O_2 (g-atom of V)⁻¹ s⁻¹ at staged-feed mode, balance He).

stants (k_1, k_2, and k_3 in Scheme 1) were obtained by solving a system of coupled differential rate equations and estimating the rate constants using standard nonlinear regression methods.[9,10]

Results and Discussion

A 2 wt % V_2O_5/Al_2O_3 catalyst with a surface density of 1.4 V nm⁻² and containing predominately monovanadate species[10] was chosen because it showed much lower k_3/k_1 ratios (~1) at 743 K (14 kPa C_2H_6, 1.7 kPa O_2) than V_2O_5 samples with higher surface densities or on other supports (e.g., ZrO_2) (k_3/k_1 >10).[2,9,10,16] The relatively high yields (~40% ethene)[10] possible with these k_3/k_1 ratios would still benefit if lower gas-phase O_2 concentrations led to even lower k_3/k_1. ODH catalysts with larger k_3/k_1 ratios (and lower ethene yields) catalyze ODH via similar pathways[16,18,19] and would similarly benefit from any effects of staging on k_3/k_1 ratios. The effects of O_2 staging were examined using a semibatch reactor that rigorously mimics a plug-flow reactor in which O_2 is introduced gradually along its axial dimension.[20,21]

C_2H_4, CO, and CO_2 formation rates were measured with 16 kPa C_2H_6 by either introducing O_2 (12.0 kPa) at the start of a batch experiment (cofeed mode) or continuously adding O_2 [4.5 mmol of O_2 (g-atom of V)⁻¹ s⁻¹] to maintain a nearly constant O_2 pressure of ~1.0 kPa throughout the experiment (staged-feed mode; 18.6 ks). In cofeed mode, O_2 concentrations decreased with time as O_2 was consumed in ODH and combustion reactions. Average O_2 concentrations were much lower in staged-feed mode than in cofeed mode (Figure 1 and Table 1), even though the same number of O_2 molecules was introduced in the two cases.

Total C_2H_6 conversion turnovers (moles of C_2H_6 converted per g-atom of V) were identical for cofeed and staged-feed modes (Figure 1), consistent with a zero-order dependence of ODH rates on O_2 pressure (Figure 2).[10,16,18] These results indicate that reoxidation of reduced V centers is rapid,[22] even at the lower O_2 pressures prevalent in staged experiments. Figure 2 shows essentially no dependence of k_3 on O_2 pressure, as was also found for k_1 and k_2 (not shown). More extensive results obtained on other supported vanadia catalysts confirmed that both k_3 and k_3/k_1 are independent of O_2 partial pressure.[23] The data in Figure 2 were obtained in a plug-flow reactor with a much larger

Table 1. Average O$_2$ Concentration and Reaction Rate Constants of C$_2$H$_6$ Dehydrogenation (k_1), C$_2$H$_6$ Combustion (k_2), and C$_2$H$_4$ Combustion (k_3) on 2 wt % VO$_x$/Al$_2$O$_3$ in a Gradientless Batch Reactor [743 K, 16.0 kPa C$_2$H$_6$, 12.0 kPa O$_2$ at Cofeed Mode; 1.0 kPa and 4.5 mmol of O$_2$ (g-atom of V)$^{-1}$ s^{-1} at Staged-Feed Mode, Balance He]

		rate constant						
				C$_2$H$_4$ combustion (s^{-1})				
	average O$_2$ concn [mol (g-atom of V)$^{-1}$]	C$_2$H$_6$ dehydrogenation (k_1, s^{-1})^a	C$_2$H$_6$ combustion (k_2, s^{-1})^a	total (k_3)^a	homogeneous^b	heterogeneous^c	k_2/k_1	k_3/k_1
cofeed	53	1.5×10^{-5}	1.1×10^{-5}	2.2×10^{-5}	0.65×10^{-5}	1.5×10^{-5}	0.72	1.4
staged feed	8.3	1.5×10^{-5}	1.1×10^{-5}	1.6×10^{-5}	0.090×10^{-5}	1.5×10^{-5}	0.72	1.0

^{a} Estimated from data in Figure 3. ^{b} Estimated from data in Figure 4. ^{c} Calculated from total C$_2$H$_4$ combustion rates constant − homogeneous C$_2$H$_4$ combustion rate constant.
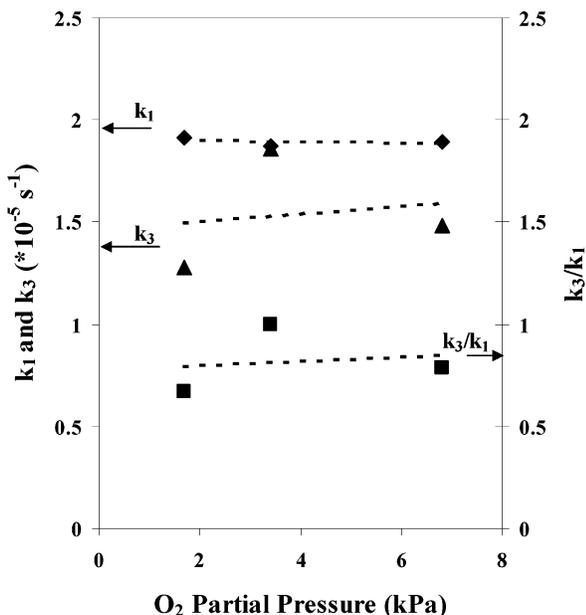
Figure 2. Dependence of C$_2$H$_6$ ODH and combustion rate constants (k_1, diamonds; k_3, triangles; k_3/k_1, squares) on the O$_2$ concentration in a flow reactor (9) [2 wt % V$_2$O$_5$/Al$_2$O$_3$ (1.4 V nm^{-2}), 743 K, 13.5 kPa C$_2$H$_6$].

catalyst-to-heated-void volume ratio than the recirculating reactor (∼0.5 vs 0.05);[10] thus, any homogeneous ethene combustion contributions would be much smaller than those in the recirculating reactor. Lattice O atoms are the most abundant reactive intermediates on VO$_x$ surfaces during ethane ODH reactions, the rates of which depend solely on kinetically relevant C−H bond activation steps.[16,22] Staged-O$_2$ experiments can be used to explore a larger range of C$_2$H$_6$ conversion than that in cofeed experiments, because cofed O$_2$ is depleted as C$_2$H$_6$ conversion occurs, while O$_2$ can be added indefinitely while maintaining any desired O$_2$ concentration by means of staging protocols.

C$_2$H$_4$, CO, and CO$_2$ selectivities and site yields are shown in Figure 3. C$_2$H$_4$ selectivity decreased with increasing C$_2$H$_6$ conversion because of sequential C$_2$H$_4$ combustion reactions (Scheme 1). Ethene site yields are slightly higher when O$_2$ coreactants are introduced gradually, and CO$_x$ site yields are correspondingly lower (Figure 3b). These effects of O$_2$ staging are small but detectable and reproducible. Creaser et al. previously observed similar O$_2$ partial pressure dependences of ODH selectivity during cofeed studies of propane ODH on V−Mg−O catalysts.[24] Both of these results seem at first to contradict the previous conclusions that heterogeneous oxidation kinetics for both primary and secondary steps do not depend on O$_2$ concentration, because the concentration of lattice O atoms is at saturation and
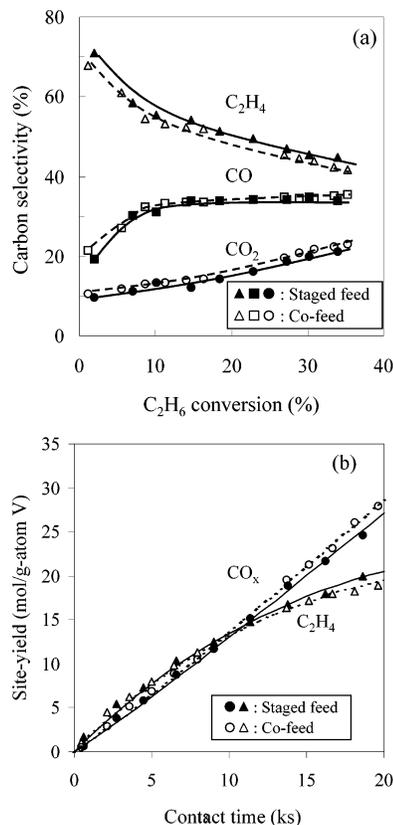
Figure 3. (a) Selectivity of C$_2$H$_6$ (triangles), CO (squares), and CO$_2$ (circles) on a carbon basis during C$_2$H$_6$ ODH on 2 wt % V$_2$O$_5$/Al$_2$O$_3$ in a gradientless batch reactor [743 K, 16.0 kPa C$_2$H$_6$, 12.0 kPa O$_2$ at cofeed mode; 1.0 kPa and 4.5 mmol of O$_2$ (g-atom of V)$^{-1}$ s^{-1} at staged-feed mode, balance He]. (b) Site yield of C$_2$H$_6$ (triangles) and CO$_x$ (circles) during C$_2$H$_6$ ODH on 2 wt % V$_2$O$_5$/Al$_2$O$_3$ in a gradientless batch reactor [743 K, 16.0 kPa C$_2$H$_6$, 12.0 kPa O$_2$ at cofeed mode; 1.0 kPa and 4.5 mmol of O$_2$ (g-atom of V)$^{-1}$ s^{-1} at staged-feed mode, balance He].

independent of prevalent O$_2$ pressures. Creaser et al. originally proposed that an alternate combustion pathway, not associated with Scheme 1, was active to explain this O$_2$ dependence.[24] They simulated the O$_2$ dependence of propane ODH using two different types of surface species, one of which was active for ODH and the other of which was active for deep combustion.[25] Our results, however, are not consistent with two types of surface oxygen on VO$_x$/Al$_2$O$_3$. Isotopic labeling experiments with reactant mixtures of C$_2$H$_6$/^{16}O$_2$/^{18}O$_2$ on V^{16}O$_x$/Al$_2$^{16}O$_3$ in a recirculating batch reactor showed that the ^{18}O/^{16}O ratio in both the H$_2$O (formed during both ODH and combustion reactions) and CO$_x$ products was similar at all contact times, indicating that ODH and combustion reactions sample the same lattice oxygen pool, which suggests that similar sites are involved in ODH and combustion reactions.[19] A more
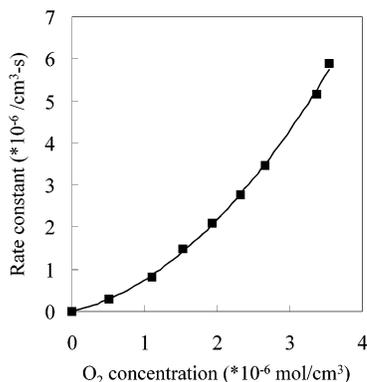
Figure 4. Homogeneous C_2H_4 combustion rate constant normalized by the reactor heated volume (2.0 cm^3) as a function of the O_2 concentration [743 K, 16.0 kPa C_2H_4, 0.13 μmol s^{-1} O_2, balance He, in a gradientless batch reactor].

rigorous kinetic analysis of our present results, described below, shows instead that these beneficial effects of O_2 staging reflect the nonzero O_2 dependence of homogeneous C_2H_4 combustion pathways. In effect, we find that O_2 staging influences C_2H_6 ODH selectivity only when reaction temperatures or reactor configurations lead to a detectable loss of C_2H_4 selectivity via gas-phase reactions between C_2H_4 and O_2 to form CO and CO_2.

Rate constants for each step in Scheme 1 were estimated using nonlinear regression methods from data in Figure 3 for both O_2 introduction modes and batch reactor mole balance equations for all species;[9] the analysis assumes first-order rate dependences on C_2H_6 or C_2H_4 and zero-order dependence on O_2. These rate constants (k_1, k_2, and k_3) and the corresponding selectivities are shown in Table 1. C_2H_6 dehydrogenation (k_1) and combustion (k_2) rate constants are the same for both O_2 feed modes, but C_2H_4 combustion rate constants (k_3) are larger in cofeed mode (2.2×10^{-5} s^{-1}) than in staged-feed (1.6×10^{-5} s^{-1}) mode. The k_2/k_1 and k_3/k_1 values in Table 1 are slightly larger than those estimated previously (0.38 and 0.67, respectively) from plug-flow reactor cofeed experiments restricted to very low C_2H_6 conversions ($\sim$2%) using a linearized version of the batch reactor equations.[10] Considering only the low conversion (<5%) cofeed data in Figure 1, the recirculating reactor k_2/k_1 value of 0.39 agrees with plug-flow reactor results, but the k_3/k_1 value of $\sim$1.8 is significantly higher than that in the plug-flow reactor because of contributions from homogeneous ethene combustion pathways (Figure 4), as a result of much smaller catalyst-to-void volume ratios in the recirculating reactor ($\sim$0.05 vs $\sim$0.5).

Homogeneous C_2H_4 combustion contributions were examined by measuring the effect of O_2 concentration on C_2H_4 reaction rates using an empty reactor with the same heated volume as that in catalytic tests (2.0 cm^3). Continuous O_2 introduction was used in order to increase O_2 concentrations gradually with time, while C_2H_4 (16.0 kPa) was circulated through the empty reactor. Pseudo-first-order homogeneous ethene combustion rate constants (K'_3) increased sharply with increasing O_2 concentration (Figure 4). This contrasts the zero-order O_2 dependence of all heterogeneous reactions in Scheme 1 (Figure 2).

The homogeneous ethene combustion rates predicted from these data for the respective average O_2 concentrations in staged-feed and cofeed modes are shown in

Table 1. Heterogeneous ethene combustion rates, derived by subtracting the corresponding homogeneous rates from measured rates, are also shown. Homogeneous ethene combustion rates in cofeed mode are about 7 times higher than those in staged-feed mode (6.5×10^{-6} vs 9.0×10^{-7} s^{-1}). In contrast, heterogeneous (catalytic) ethene combustion rates are identical in the two modes (1.5×10^{-5} vs 1.5×10^{-5} s^{-1}), consistent with the saturated oxide surfaces prevalent for both O_2 feed modes and with the zero-order O_2 kinetics for all reaction steps in Scheme 1.

We conclude that staging O_2 coreactants minimizes its average concentration while supplying stoichiometric ODH requirements, and it decreases the homogeneous contributions to ethene combustion rates. Primary and secondary *catalytic* pathways are not influenced by the mode of oxygen introduction or by the average O_2 partial pressures in the range of the study (1.0−12.0 kPa). Thus, the benefits of staging O_2 coreactants will be observed only when reaction conditions or reactor designs lead to detectable contributions from homogeneous ethene combustion reactions.

We also note that the benefits of O_2 staging or membrane reactors, which reflect only the kinetic inhibition of homogeneous alkene combustion pathways, may well disappear as staging is implemented in large-scale reactors, for which catalyst-to-heated-void volumes are significantly higher than those in laboratory reactors. As a result, homogeneous pathways become less important than catalytic reactions in practical applications than in laboratory concept demonstrations. Typical catalyst-to-void volume ratios in large tubular reactors are 1−2, while laboratory reactors have much smaller ratios (e.g., $\sim$0.5 for our tubular reactor and 0.05 for our recirculating reactor). The ratio of homogeneous to heterogeneous ethene combustion rates in our laboratory recirculating reactor is 0.43 at 743 K; the corresponding ratio in a large tubular reactor with a catalyst-to-volume ratio of unity would be only 0.01−0.02. Thus, the benefits of staging using multiple injectors or membranes would be commensurately smaller in large-scale applications. Such considerations are essential in placing staging strategies within an accurate context for ODH reactions and for other reactions involving redox cycles with lattice oxygen atoms as the most abundant reactive intermediates.

Conclusions

Staged-oxygen injection and oxygen cofeed experiments have shown that the kinetics of ethane ODH on a VO$_x$/Al$_2$O$_3$ catalyst are identical. In both cases, the dependencies of ethane ODH, ethane combustion, and ethene combustion are zero order with respect to oxygen concentration. However, the oxygen cofeed experiments reveal a contribution to the ethene combustion from homogeneous combustion, which increases with increasing O_2 partial pressure. The importance of this process is directly proportional to the ratio of catalyst-to-reactor-void volumes and can become important when this ratio is low or at high reaction temperatures. Because the catalyst-to-void volume in a commercial reactor system is high (1−2), the results of the present investigation suggest that there would be little justification for the mechanical complexities of a plug-flow reactor with staged-oxygen injection or operated in a cyclic mode or the inherent difficulties associated with obtaining and operating a suitable membrane reactor.

Literature Cited

(1) Mars, P.; van Krevelen, D. W. Oxidations carried out by means of vanadium oxide catalysts. *Chem. Eng. Sci.* **1954**, *3*, Special Suppl., 41.

(2) Kung, H. H. Oxidative dehydrogenation of light (C_2 to C_6) alkanes. *Adv. Catal.* **1994**, *40*, 1.

(3) Mamedov, E. A.; Cortés Corberán, V. Oxidative dehydrogenation of lower alkanes on vanadium oxide-based catalysts—the present state-of-the-art and outlooks. *Appl. Catal. A* **1995**, *127*, 1.

(4) Albonetti, S.; Cavani, F.; Trifirò, F. Key aspects of catalyst design for the selective oxidation of paraffins. *Catal. Rev.—Sci. Eng.* **1996**, *38*, 413.

(5) Vrieland, G. E.; Murchison, C. B. Anaerobic oxidation of butane to butadiene over magnesium molybdate catalysts. 1. Magnesia supported catalysts. *Appl. Catal. A* **1996**, *134*, 101.

(6) Creaser, D.; Andersson, B.; Hudgins, R. R.; Silveston, P. L. Transient kinetic analysis of the oxidative dehydrogenation of propane. *J. Catal.* **1999**, *182*, 264.

(7) Creaser, D.; Andersson, B.; Hudgins, R. R.; Silveston, P. L. Transient study of oxidative dehydrogenation of propane. *Appl. Catal. A* **1999**, *187*, 147.

(8) Ballarini, N.; Cavani, F.; Ferrari, M.; Catani, R.; Cornaro, U. Oxydehydrogenation of propane catalyzed by V−Si−O cogels: enhancement of the selectivity to propylene by operation under cyclic conditions. *J. Catal.* **2003**, *213*, 95.

(9) Khodakov, A.; Yang, J.; Su, S.; Iglesia, E.; Bell, A. T. Structure and properties of vanadium oxide zirconia catalysts for propane oxidative dehydrogenation. *J. Catal.* **1998**, *177*, 343.

(10) Argyle, M. D.; Chen, K. D.; Bell, A. T.; Iglesia, E. Effect of catalyst structure on oxidative dehydrogenation of ethane and propane on alumina-supported vanadia. *J. Catal.* **2002**, *208*, 139.

(11) Tonkovich, A. L. Y.; Zilka, J. L.; Jimenez, D. M.; Roberts, G. L.; Cox, J. L. Experimental investigations of inorganic membrane reactors: A distributed feed approach for partial oxidation reactions. *Chem. Eng. Sci.* **1996**, *51*, 789.

(12) Wang, H.; Cong, Y.; Yang, W. Continuous oxygen ion transfer medium as a catalyst for high selective oxidative dehydrogenation of ethane. *Catal. Lett.* **2002**, *84*, 101.

(13) Akin, F. T.; Lin, Y. S. Selective oxidation of ethane to ethylene in a dense tubular membrane reactor. *J. Membr. Sci.* **2002**, *209*, 457.

(14) Coronas, J.; Menendez, M.; Santamaria, J. Use of a ceramic membrane reactor for the oxidative dehydrogenation of ethane to ethylene and higher hydrocarbons. *Ind. Eng. Chem. Res.* **1995**, *34*, 4229.

(15) Takehira, K.; Shishido, T.; Sakai, N.; Shimomura, J.; Hamakawa, S.; Kajioka, H. Oxidation of lower alkanes over MoO_3−V_2O_5 supported on YSZ-aided membrane reactor. *Desalination* **2002**, *144*, 425.

(16) Chen, K. D.; Khodakov, A.; Yang, J.; Bell, A. T.; Iglesia, E. Isotopic tracer and kinetic studies of oxidative dehydrogenation pathways on vanadium oxide catalysts. *J. Catal.* **1999**, *186*, 325.

(17) Biscardi, J. A. Structure and Function of Metal Cations in Light Alkane Reactions Catalyzed by Modified H−ZSM5. Dissertation, University of California at Berkeley, Berkeley, CA, 1998.

(18) Chen, K. D.; Bell, A. T.; Iglesia, E. Kinetics and mechanism of oxidative dehydrogenation of propane on vanadium, molybdenum, and tungsten oxides. *J. Phys. Chem. B* **2000**, *104*, 1292.

(19) Argyle, M. D.; Chen, K. D.; Bell, A. T.; Iglesia, E. Ethane Oxidative Dehydrogenation Pathways on Vanadium Oxide Catalysts. *J. Phys. Chem. B* **2002**, *106*, 5421.

(20) Waku, T.; Biscardi, J. A.; Iglesia, E. Catalytic dehydrogenation of alkanes on Pt/Na−[Fe]ZSM5 and staged O_2 introduction strategies for selective H_2 removal. *J. Catal.* **2003**, accepted for publication.

(21) Fogler, H. S. *Elements of Chemical Reaction Engineering*; Prentice Hall PTR: Upper Saddle River, NJ, 1999.

(22) Argyle, M. D.; Krebs, C.; Ressini, C.; Chen, K. D.; Bell, A. T.; Iglesia, E. Measurements of reduced centers in dispersed metal oxides during alkane oxidative dehydrogenation by in situ UV−visible spectroscopy. *Chem. Commun.* **2003**, *16*, 2082.

(23) Argyle, M. D. Oxidative Dehydrogenation of Light Alkanes on Metal Oxide Catalysts. Dissertation, University of California at Berkeley, Berkeley, CA, 2003.

(24) Creaser, D.; Andersson, B.; Hudgins, R. R.; Silveston, P. L. Oxygen partial pressure effects on the oxidative dehydrogenation of propane. *Chem. Eng. Sci.* **1999**, *54*, 4365.

(25) Creaser, D.; Andersson, B.; Hudgins, R. R.; Silveston, P. L. Kinetic modeling of oxygen dependence in oxidative dehydrogenation of propane. *Can. J. Chem. Eng.* **2000**, *78*, 182.